UNCERTAINTY MODELLING IN CONFIGURATION SPACE FOR ROBOTIC MOTION PLANNING*

L. Basañez and R. Suárez

Institut de Cibernètica (UPC-CSIC), Diagonal 647, 08028 Barcelona, Spain

Abstract. The paper deals with uncertainty in the context of robot motion planning. Most of the recent robot planning approaches make use of the Configuration Space concept and include uncertainty considerations. Nevertheless, the lack of a general realistic uncertainty model is evident. In this paper we describe the uncertainty sources affecting objects manipulation with robots, and establish an uncertainty model for each one. This models are then used to determine, in Configuration Space, the configurations sets (*CU*) of possible contact in presence of uncertainty. In our approach, robot motion planners should take into account *CU* sets instead of the nominal C-surfaces of Configuration Space. The work has been done for planar movements, but it can be extended to more degrees of freedom without theoretical problems.

Keywords. Robots; Modelling; Uncertainty; Configuration Space; Planning.

INTRODUCTION

Parameters and variables describing objects or objects' behaviour in real world are not exactly known. In some robot tasks it is not enough to deal with *nominal* or *predicted* values, but some specification about their imprecision is necessary. This is the case of robot motion planning, specially when the object in the robot gripper (or the robot itself) may become in contact with others objects in the environment.

In obstacles avoidance, the uncertainty of the parameters and variables must be taken into account to warrant that contact does not occurs. On the other hand, in assembly tasks, uncertainty must be considered in order to assure parts matting success.

The uncertainty of a parameter or variable is often associated with concepts such as deviation, error, or tolerance. The difference between any two of them is subtle, and sometimes they are treated as synonyms. In this paper, we will assume the following definitions:

Definition 1: The *deviation* of a parameter or variable is the difference between the actual and the measured or calculated values.

Definition 2: The *uncertainty* of a parameter or variable is the domain containing all possible actual values for an observed one subject to deviations.

Deviations are represented here by δ and uncertainties by U, both with a subscript representative of the related variable or parameter. Parameters used to describe the uncertainty are represented by ϵ with the same subscript. The subscript o indicates *observed* values, sensed or calculated. This nomenclature is valid for both scalar and vectorial quantities.

There are a considerable number of works dealing with robot motion planning. Several of them include some analysis of uncertainty, but each one uses a different uncertainty model according to its own approach (Brooks, 1982; Xiao and Volz, 1988; Buckley, 1989). Nevertheless, the necessity of a general realistic uncertainty model is becoming patent.

Configuration Space (Lozano Perez, 1983) is a basic tool for fine-motion planning, and from that the necessity of modelling uncertainty in it. An atypical approach is the proposed by Donald (1988) who includes uncertainty by increasing the dimension of the Configuration Space.

In this paper we develop a model of uncertainty for a three degrees of freedom problem (two degrees of freedom of translation and one of rotation), but it can be easily extended to more degrees of freedom. This model has been developed for a fine-motion planner which takes into account uncertainties affecting contact configurations, force measurements and velocity of the moving object. A first description of the planner can be found in Suárez and Basañez (1989).

In this work it is assumed that the objects are rigid and polyhedral. Thus when they move with the three above mentioned degrees of freedom, can be considered "planar" polygonal objects.

UNCERTAINTY SOURCES

Strictly speaking, uncertainty always arises from a measurement process. So, uncertainty has always sensorial origin, and it is propagated as the measured values are used to calculate another ones (theory of errors). Nevertheless, it is often possible to consider and model higher level uncertainty sources for some specific purposes. In the following subsections, uncertainty sources related with fine-motion planning are described.

Uncertainty of the shape and size of objects

Uncertainty of the objects shape and size is due to their manufacturing tolerances. These tolerances can be specified by techniques called *geometric tolerancing* which allows to limit the possible real objects that can be considered as instances of a nominal one described by a nominal model. Requicha (1983), Jayaraman and Srinivasan (1989), and Fleming (1989) deal with the problem of geometrically toleranced parts representation.

*This work was partially supported by Comision Interministerial de Ciencia y Tecnologia (CICYT) under the project ROB 89-0287

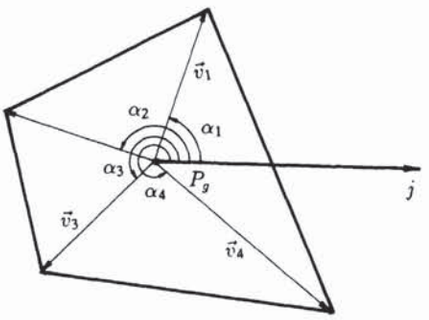

Figure 1: Description of a object using a point P_g and an axis j as reference

Following Requicha (1983), we will consider for each object a *Datum System* formed by an object reference point P_g and an axis j that has P_g as origin (both defined in an appropriate Master Datum System). Taking P_g and j as reference, the object is described by specifying each vertex position by means of a vector $\vec{v}$ (Fig. 1).

With this nominal object model, vertex position uncertainty can be expressed

$$U_v = \{\vec{v} \mid \|\vec{v} - \vec{v}_o\| \leq \epsilon_v\} \quad (1)$$

where $\vec{v}$ represent the real position of the vertex, $\vec{v}_o$ the predicted position, and U_v the corresponding uncertainty. Uncertainty of the position of a any point of the object boundary can be modelled by a similar expression. It is also assumed that the object boundary satisfies an additional slow-variation condition.

Uncertainty of the position measurement of a point of a static object

This uncertainty entirely depends on the sensors or measurement system used to locate the point, but a generic model can be established as

$$U_m = \{\vec{a} \mid \|\vec{a} - \vec{a}_o\| \leq \epsilon_m\} \quad (2)$$

where $\vec{a}$ represents the real position of the point, $\vec{a}_o$ the observed position and U_m its uncertainty.

Uncertainty of the configuration of a static object

Depending on the way the configuration is obtained, three differents situations are possible:

1) *The object configuration is known a priori.* For instance, when the object is placed in the work environment by a feeder system. Being desirable an uncertainty model independent of any specific feeder, the simplest way is to assume that each object vertex is located inside a circle of radius ϵ_{p_r} centered in the vertex predicted position. From this assumption, it follows that every object point, including the object reference point, is constrained to be inside a circle of the same radius, and the object orientation uncertainty can then be ignored. This model will be adopted in this paper.

2) *The object configuration is observed on-line.* The configuration uncertainty could be described by two parameters: ϵ_{p_r}, affecting the position of the object reference point, and ϵ_{ϕ_r}, affecting the orientation around that point. Both parameters will be independents if the object position and orientation are determined without identify any particular point, and dependents otherwise. In the first case, the region in which an object point can actually be, is swept by a circle of radius ϵ_{p_r} rotating an angle ϵ_{ϕ_r} around the reference point; in the second case, regions shape and size depend on the particular points observed.

3) *The object configuration is known because the object has been placed by the robot.* If the object has been previously manipulated only once by the robot, the uncertainty model is represented by two independent parameters ϵ_{p_r} and ϵ_{ϕ_r}, this last now representing the uncertainty of the object orientation around the grasping point. If the object has been manipulated several times by the robot, configuration uncertainty results from the application of the same principle in an accumulative way.

Uncertainty of the robot positioning

Although a lot of factors influence the uncertainty of the robot end effector positioning (Day, 1988), joints position deviations can be considered as the main one. Uncertainty of each joint position could be individually determined by considering the particular robot elements (servomechanism type, gears, position sensing and feedback, etc). Nevertheless, modelling the end effector uncertainty from them, often gives rise to a non-linear function of the robot configuration (Benhabib, Fenton and Goldenberg, 1987). Since joint position deviation is of the same order than its resolution, the Jacobian of the manipulator can be used to approximate the end effector positioning uncertainty, but maintaining the configuration dependency. In order to avoid this dependency, a generic model can be directly established for the robot end effector positioning.

Robot precision is usually specified by two parameters, representing the maximum distance and angle that position and orientation of the robot end effector can defer from the predicted values. The same parameters can also be chosen to specify position and orientation uncertainty, that is,

$$U_{p_r} = \{\vec{p}_r \mid \|\vec{p}_r - \vec{p}_{ro}\| \leq \epsilon_{p_r}\} \quad (3)$$

$$U_{\phi_r} = \{\phi_r \mid |\phi_r - \phi_{ro}| \leq \epsilon_{\phi_r}\} \quad (4)$$

where $\vec{p}_r$ and ϕ_r represent the real position and orientation of the end effector and $\vec{p}_{ro}$ and ϕ_{ro} their observed values. In this model, the position uncertainty is independent of the orientation uncertainty, although they both depend on joint position uncertainties.

Slide of the object in the gripper

Undesired slide can be strongly reduced by using an adequate gripper and making a correct grasp planning, uncertainty due to other sources being also reduced in this way. In this work, we model the slide of the object in the gripper assuming upper limits for translation, ϵ_{p_d}, and for rotation around the grasping point, ϵ_{o_d}.

UNCERTAINTY OF THE ABSOLUTE POSITION OF ANY OBJECT POINT

In order to predict a possible contact configuration it is necessary to consider the uncertainty of the absolute location of the objects boundary. This can be done by determining the uncertainty of the absolute position of each boundary point. Uncertainty sources are different for a static object lying in the work environment and for a grasped object fixed in the robot gripper.

Static object

Depending on how the position of a point is estimated, the two following cases are possibles:

1. Computing from a nominal object model and the object configuration. Uncertainty comes from deviations of the object shape and size (δ_v) and from the deviation of the object configuration (δ_{p_p}).

   With the proposed models both deviations can be added, $\delta_a = \delta_v + \delta_{p_p}$. Then, the maximum deviation is $\epsilon_a = \epsilon_v + \epsilon_{p_p}$.

2. Direct observation of the point position by a sensor external to the robot. Uncertainty comes from the measurement deviation of the observation system (δ_m); then $\delta_a = \delta_m$.

The *absolute position of a vertex of a static object* will be represented by

$$\vec{a} = \vec{a}_o + \vec{\delta}_a = \begin{bmatrix} a_{xo} + \delta_a \cos\theta_a \\ a_{yo} + \delta_a \sin\theta_a \end{bmatrix} \tag{5}$$

The *absolute position of a point of a static object edge* limited by vertices $\vec{a}_1$ and $\vec{a}_2$, will be given by

$$\vec{a} = \vec{a}_1 + k(\vec{a}_2 - \vec{a}_1) = \vec{a}_{1o} + k(\vec{a}_{2o} - \vec{a}_{1o}) + \vec{\delta}_a =$$
$$= \begin{bmatrix} a_{1xo} + k(a_{2xo} - a_{1xo}) + \delta_a \cos\theta_a \\ a_{1yo} + k(a_{2yo} - a_{1yo}) + \delta_a \sin\theta_a \end{bmatrix} \tag{6}$$

where $k \in [0, 1]$.

Grasped object

The deviations bringing about from the following three sources are to be considered:

- deviations of the object shape and size (δ_v)
- deviations of the position and orientation of the robot end effector (δ_{p_r} and δ_{ϕ_r})
- deviations of the position and orientation of the object in the gripper, which are due to:
  - deviations of the object configuration before it was grasped (δ_{p_p})
  - deviations of the position and orientation of the robot end effector during the grasping (δ_{p_r} and δ_{ϕ_r})
  - slides of the object in the gripper (δ_{p_d} and δ_{ϕ_d})

  The deviation of the position of the object in the gripper can be summarize as $\delta_{p_g} = \delta_{p_r} + \delta_{p_p} + \delta_{p_d}$. Then the maximum deviation is $\epsilon_{p_g} = \epsilon_{p_r} + \epsilon_{p_p} + \epsilon_{p_d}$. Since δ_{ϕ_r} and δ_{ϕ_d} are referred to the same rotation point, the deviation of the orientation of the object in the gripper can be summarized as $\delta_{\phi_g} = \delta_{\phi_r} + \delta_{\phi_d}$, with the maximum value $\epsilon_{\phi_g} = \epsilon_{\phi_r} + \epsilon_{\phi_d}$.

The *absolute position of a vertex of the grasped object* will be given by (Fig. 2)

$$\vec{b} = \vec{p}_r + \vec{p}_g + \vec{v} =$$
$$= \begin{bmatrix} p_{r_xo} + h\cos(\phi_{ro} + \phi_{go} + \delta_{\phi_r\phi_g} + \gamma) + \delta_{p_rp_gv}\cos\theta_{p_rp_gv} \\ p_{r_yo} + h\sin(\phi_{ro} + \phi_{go} + \delta_{\phi_r\phi_g} + \gamma) + \delta_{p_rp_gv}\sin\theta_{p_rp_gv} \end{bmatrix} \tag{7}$$

where

$$h = \sqrt{p_g^2 + v^2 + 2p_gv\cos(\phi_m + \alpha)} \tag{8}$$

$$\gamma = \arcsin\left(\frac{v}{h}\sin(\phi_m + \alpha)\right) \tag{9}$$

and

$$\epsilon_{\delta_{p_rp_gv}} = \epsilon_{p_r} + \epsilon_{p_g} + \epsilon_v \tag{10}$$

$$\epsilon_{\phi_r\phi_g} = \epsilon_{\phi_r} + \epsilon_{\phi_g} \tag{11}$$

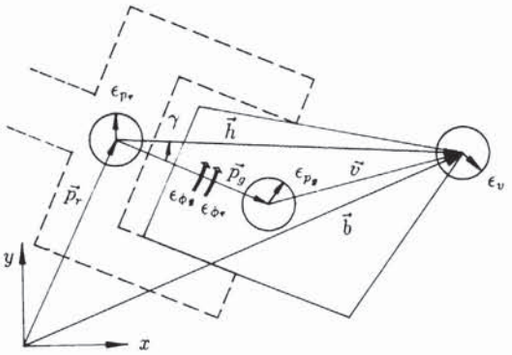

Figure 2: Absolute position of a vertex of a grasped object

The *absolute position of a point of a grasped object edge* limited by vertices $\vec{b}_1$ and $\vec{b}_2$ can be expresed

$$\vec{b} = \vec{b}_1 + k(\vec{b}_2 - \vec{b}_1) =$$
$$= \begin{bmatrix} p_{r_xo} + h_1\cos(\phi_{ro} + \phi_{go} + \delta_{\phi_r\phi_g} + \gamma_1) + \delta_{p_rp_gv}\cos\theta_{p_rp_gv} + \\ k(h_2\cos(\phi_{ro} + \phi_{go} + \delta_{\phi_r\phi_g} + \gamma_2) - h_1\cos(\phi_{ro} + \phi_{go} + \delta_{\phi_r\phi_g} + \gamma_1)) \\ \\ p_{r_yo} + h_1\sin(\phi_{ro} + \phi_{go} + \delta_{\phi_r\phi_g} + \gamma_1) + \delta_{p_rp_gv}\sin\theta_{p_rp_gv} + \\ k(h_2\sin(\phi_{ro} + \phi_{go} + \delta_{\phi_r\phi_g} + \gamma_2) - h_1\sin(\phi_{ro} + \phi_{go} + \delta_{\phi_r\phi_g} + \gamma_1)) \end{bmatrix} \tag{12}$$

where $k \in [0, 1]$ and equations (10) and (11) also apply.

UNCERTAINTY IN THE CONFIGURATION SPACE

In order to build C-surfaces in Configuration Space we choose a reference point fixed to the gripper (the TCP point) represented by $\vec{p}_r$ in the absolute reference system. The three degrees of freedom will be indicated by p_{rx}, p_{ry} and $\rho\phi_r$, where ρ is a constant with units of length. Since the numerical value of ρ is not critical for this analysis, it can be taken as unitary and thus a point of Configuration Space is directly represented by $[p_{rx}\ \ p_{ry}\ \ \phi_r]^T$.

Two basic kinds of contact are possibles between polygonal objects in the plane: *type-1* when a vertex of the moved object touch an edge of a static object, and *type-2* when an edge of the moved object touch a vertex of a static object. Each type of contact generates in the 3-dimensional Configuration Space an associated C-surface, which is also called *type-1* or *type-2* C-surface and represents all the configurations in which such basic contact occurs. Since C-surfaces in absence of uncertainty are a well known subject, in this section we will develop expressions for C-surfaces including uncertainty, that is, we will determine all the configurations in which a certain kind of contact may be possible.

Type-1 C-surfaces. A grasped object vertex $\vec{b}$ is in contact with a point $\vec{a}$ of a static object edge; this condition success if $\vec{a} = \vec{b}$. From expressions (6) and (7) it results

$$\begin{cases} p_{r_xo} + h\cos(\phi_{ro} + \phi_{go} + \delta_{\phi_r\phi_g} + \gamma) + \delta_{p_rp_gv}\cos\theta_{p_rp_gv} = \\ \qquad a_{1xo} + k(a_{2xo} - a_{1xo}) + \delta_a\cos\theta_a \\ p_{r_yo} + h\sin(\phi_{ro} + \phi_{go} + \delta_{\phi_r\phi_g} + \gamma) + \delta_{p_rp_gv}\sin\theta_{p_rp_gv} = \\ \qquad a_{1yo} + k(a_{2yo} - a_{1yo}) + \delta_a\sin\theta_a \end{cases} \tag{13}$$

By eliminating k, a family of type-1 C-surfaces parametrized in the deviations could be obtained.

Type-2 C-surfaces. A point $\vec{b}$ of a grasped object edge is in contact with a vertex $\vec{a}$ of a static object; this condition success if $\vec{a} = \vec{b}$. From expressions (5) and (12) it results

$$\begin{cases} a_{x_o} + \delta_a \cos\theta_a = \\ p_{r_{x_o}} + h_1 \cos(\phi_{r_o} + \phi_{g_o} + \delta_{\phi_r\phi_g} + \gamma_1) + \delta_{p_rp_gv} \cos\theta_{p_rp_gv} + \\ k(h_2 \cos(\phi_{r_o} + \phi_{g_o} + \delta_{\phi_r\phi_g} + \gamma_2) - h_1 \cos(\phi_{r_o} + \phi_{g_o} + \delta_{\phi_r\phi_g} + \gamma_1)) \\ \\ a_{y_o} + \delta_a \sin\theta_a = \\ p_{r_{y_o}} + h_1 \sin(\phi_{r_o} + \phi_{g_o} + \delta_{\phi_r\phi_g} + \gamma_1) + \delta_{p_rp_gv} \sin\theta_{p_rp_gv} + \\ k(h_2 \sin(\phi_{r_o} + \phi_{g_o} + \delta_{\phi_r\phi_g} + \gamma_2) - h_1 \sin(\phi_{r_o} + \phi_{g_o} + \delta_{\phi_r\phi_g} + \gamma_1)) \end{cases} \tag{14}$$

By eliminating k, a family of type-2 C-surfaces parametrized in the deviations could be obtained.

The families of type-1 and type-2 C-surfaces contain all possible contact configurations *(Cc)* in presence of uncertainty. When planning robot movements using the Configuration Space approach, this set of configurations must be considered instead of the nominal C-surfaces.

In order to obtain *Cc* it is necessary to determine the envelopes of the C-surfaces families. Applying the general procedure to find envelopes gives rise to algebraic expressions difficult to manipulate (e.g. in type-2 family it is necessary to solve quartic equations), thus we determine them with the help of a graphical analysis. The following nomenclature will be used

Uv : uncertainty of the position of a point of the grasped object for a given p_{r_o} and ϕ_{r_o}.

Ul : uncertainty of the position of an edge of the grasped object for a given p_{r_o} and ϕ_{r_o}.

CUv : uncertainty of the configuration of a contact between a given point of the static object and a given point of the grasped object for a given ϕ_{r_o}.

CUl : uncertainty of the configurations of a contact between a given pair vertex-edge for a given ϕ_{r_o}.

CU : uncertainty of the configurations of a contact between a given pair vertex-edge. The union of *CU*'s of every possible basic contact is equal to *Cc*.

Envelope of a family of type-1 C-surfaces

Considering that vertex $\vec{b}$ become in contact with edge l_a, the envelope is obtained in four steps by determining:

1. *Uv* of vertex $\vec{b}$.
2. *CUv* of $\vec{b}$ and $\vec{a} \in l_a$.
3. *CUl* of $\vec{b}$ and l_a.
4. *CU* of $\vec{b}$ and l_a.

Step 1. As it is shown in Fig. 3, *Uv* is limited by four arcs of circumference. The circumferences are

$$\begin{cases} x = p_{r_{x_o}} + \left(h + \eta\, \epsilon_{p_rp_gv}\right) \cos\theta_{R_r} \\ y = p_{r_{y_o}} + \left(h + \eta\, \epsilon_{p_rp_gv}\right) \sin\theta_{R_r} \end{cases} \tag{15}$$

$$\begin{cases} x = p_{r_{x_o}} + h \cos(\phi_{r_o} + \phi_{g_o} + \eta\, \epsilon_{\phi_r\phi_g} + \gamma) + \epsilon_{p_rp_gv} \cos\theta_{p_rp_gv} \\ y = p_{r_{y_o}} + h \sin(\phi_{r_o} + \phi_{g_o} + \eta\, \epsilon_{\phi_r\phi_g} + \gamma) + \epsilon_{p_rp_gv} \sin\theta_{p_rp_gv} \end{cases} \tag{16}$$

The two circumferences given by (15) for $\eta = 1, -1$ are called Cr_M and Cr_m respectively. Likewise, those given by (16) are called Cg_M and Cg_m.

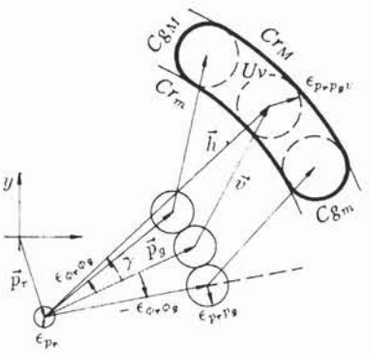

Figure 3: *Uv* of a vertex

The valid arcs of these circumferences satisfy:

$$|\phi_{r_o} + \phi_{g_o} + \gamma - \theta_{R_r}| < \epsilon_{\phi_r\phi_g} \quad \text{for } Cr_M \text{ and } Cr_m \tag{17}$$

$$-\pi < \phi_{r_o} + \phi_{g_o} + \gamma + \epsilon_{\phi_r\phi_g} - \theta_{p_rp_gv} < 0 \quad \text{for } Cg_M \tag{18}$$

$$0 < \phi_{r_o} + \phi_{g_o} + \gamma - \epsilon_{\phi_r\phi_g} - \theta_{p_rp_gv} < \pi \quad \text{for } Cg_m \tag{19}$$

Step 2. *CUv* is determined by applying a contact condition between *Uv* and a point $\vec{a}$ of l_a. The boundary of *CUv* is obtained by equaling the boundary of *Uv* to the expression of $\vec{a}$ supplied by equation (6), and solving for the position of the reference point. Since $\vec{a}$ is affected by uncertainty, the result is a set of configurations and its external envelope conforms the boundary of *CUv*.

CUv has the same shape (but not same size) of *Uv* and therefore its boundary is also composed by four arcs of circumference. The circumferences are

$$\begin{cases} p_{r_{x_o}} = a_{1x_o} + k(a_{2x_o} - a_{1x_o}) + (h + \eta(\epsilon_{p_rp_gv} + \epsilon_a)) \cos\theta_{R_{ra}} \\ p_{r_{y_o}} = a_{1y_o} + k(a_{2y_o} - a_{1y_o}) + (h + \eta(\epsilon_{p_rp_gv} + \epsilon_a)) \sin\theta_{R_{ra}} \end{cases} \tag{20}$$

$$\begin{cases} p_{r_{x_o}} = a_{1x_o} + k(a_{2x_o} - a_{1x_o}) - h \cos(\phi_{r_o} + \phi_{g_o} + \eta\, \epsilon_{\phi_r\phi_g} + \gamma) + \\ \qquad (\epsilon_{p_rp_gv} + \epsilon_a) \cos\theta_{p_rp_gva} \\ p_{r_{y_o}} = a_{1y_o} + k(a_{2y_o} - a_{1y_o}) - h \sin(\phi_{r_o} + \phi_{g_o} + \eta\, \epsilon_{\phi_r\phi_g} + \gamma) + \\ \qquad (\epsilon_{p_rp_gv} + \epsilon_a) \sin\theta_{p_rp_gva} \end{cases} \tag{21}$$

The two circumferences given by (20) for $\eta = 1, -1$ are called CCr_M and CCr_m, respectively. Likewise, those given by (21) are called CCg_M and CCg_m. It is possible that the radius of CCr_m be negative, then it has no physical sense and CCr_m is not part of the *CUv* boundary.

The valid arcs of these circumferences satisfy:

$$|\phi_{r_o} + \phi_{g_o} + \gamma + \pi - \theta_{R_{ra}}| < \epsilon_{\phi_r\phi_g} \quad \text{for } CCr_M \text{ and } CCr_m \tag{22}$$

$$0 < \phi_{r_o} + \phi_{g_o} + \gamma + \epsilon_{\phi_r\phi_g} - \theta_{p_rp_gva} < \pi \quad \text{for } CCg_M \tag{23}$$

$$-\pi < \phi_{r_o} + \phi_{g_o} + \gamma - \epsilon_{\phi_r\phi_g} - \theta_{p_rp_gva} < 0 \quad \text{for } CCg_m \tag{24}$$

Step 3. *CUl* is the zone swept by *CUv* when k varies from 0 to 1. This is equivalent to consider contact between the point $\vec{b}$ and every point of the edge l_a. The boundary of *CUl* is formed by parts of the boundaries of the *CUv* of the two vertices of l_a ($k = 0$ and $k = 1$), and by two straight segments parallel to l_a (Fig. 4). These two segments lie on two straight lines tangents to *CUv* of any point of l_a. Since the two lines are parallel to the edge l_a, they are determined by two parameters d_e and d_i respectively, such that $|d_e|$ and $|d_i|$ are the distances from each line to l_a and the signs indicate if they are on the free space side of l_a (positive sign) or on the object side of l_a (negative

sign). For ψ_{n_a} indicating the direction orthogonal to l_a pointing outside the object, d_e and d_i are determined by

$$d_e = h\cos(\psi_{n_a} - \phi_{ro} - \phi_{go} - \gamma + \eta\,\epsilon_{\phi_r\phi_g}) + \epsilon_{p_rp_gva} \quad (25)$$

$$d_i = h\cos(\psi_{n_a} - \phi_{ro} - \phi_{go} - \gamma - \eta\,\epsilon_{\phi_r\phi_g}) - \epsilon_{p_rp_gva} \quad (26)$$

with

$$\eta = 1 \quad \text{if} \quad 0 < \psi_{n_a} - \phi_{ro} - \phi_{go} - \gamma < \pi \quad (27)$$

$$\eta = -1 \quad \text{if} \quad -\pi < \psi_{n_a} - \phi_{ro} - \phi_{go} - \gamma < 0 \quad (28)$$

except for the two following particular cases:

$$\text{if } |\phi_{ro} + \phi_{go} + \gamma - \psi_{n_a} + \pi| < \epsilon_{\phi_r\phi_g} \text{ then } d_e = h + \epsilon_{p_rp_gv} + \epsilon_a \quad (29)$$

$$\text{if } |\phi_{ro} + \phi_{go} + \gamma - \psi_{n_a}| < \epsilon_{\phi_r\phi_g} \text{ then } d_i = -(h + \epsilon_{p_rp_gv} + \epsilon_a) \quad (30)$$

Step 4. *CUl* is a two dimensional cut of *CU* for a certain ϕ_{ro}, then the boundary of *CU* can be obtained from the boundary of *CUl* by varying ϕ_{ro} within a given range.

Let L_a, L_{b1}, L_{b2} be the nominal lengths of edges l_a, l_{b1} and l_{b2} (l_{b1} and l_{b2} are the edges that joint in $\vec{b}$ following the object boundary counterclokwise). The maximum deviations of the corresponding external normal directions will be

$$\epsilon_{\psi_{n_a}} = 2\epsilon_a/L_a \quad (31)$$

$$\epsilon_{\psi_{n_{b1}}} = 2\epsilon_a/L_{b1} \quad (32)$$

$$\epsilon_{\psi_{n_{b2}}} = 2\epsilon_a/L_{b2} \quad (33)$$

Let ϕ_{ro_M} and ϕ_{ro_m} be the predicted maximum and minimum values of ϕ_{ro} without uncertainty. The range of variation of ϕ_{ro} will be extended, due to uncertainty, to

$$\phi_{ro_m} - \epsilon_{\psi_{n_{b1}}} - \epsilon_{\psi_{n_a}} - \epsilon_{\phi_r} - \epsilon_{\phi_g} < \phi_{ro} < \phi_{ro_M} + \epsilon_{\psi_{n_{b2}}} + \epsilon_{\psi_{n_a}} + \epsilon_{\phi_r} + \epsilon_{\phi_g} \quad (34)$$

Envelope of a family of type-2 C-surfaces

Considering that edge l_b become in contact with vertex $\vec{a}$, the envelope is obtained in four steps by determining:

1. *Uv* of vertices $\vec{b}_1$ and $\vec{b}_2$ of l_b.
2. *Ul* of l_b.
3. *CUl* of l_b and $\vec{a}$.
4. *CU* of l_b and $\vec{a}$.

Step 1. Determination of *Uv* of $\vec{b}_1$ and $\vec{b}_2$ is done in the same way as in step 1 of type-1 C-surfaces.

Step 2. Two cases are possibles depending on the relative positions of l_b and the reference point in absence of uncertainty. We will call case A when the line orthogonal to l_b through the reference point intersects l_b, and case B otherwise. As it is shown in Fig. 5 and Fig. 6 the boundary of *Ul* is composed by

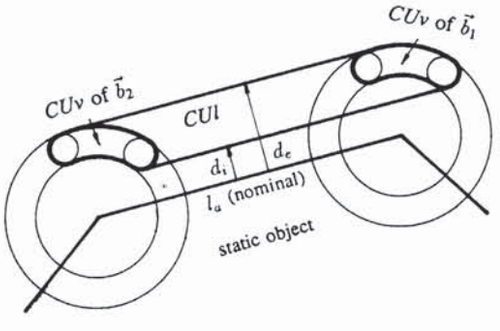

Figure 4: *CUl* of type-1 contact

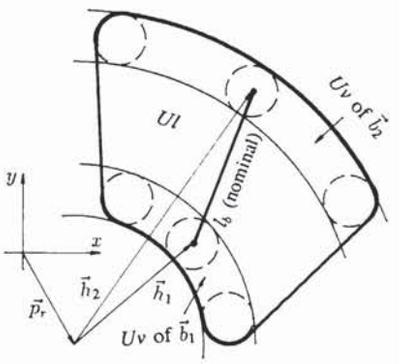

Figure 5: *Ul* of type-2 contact (case A)

part of the boundary of *Uv* of $\vec{b}_1$, part of the boundary of *Uv* of $\vec{b}_2$, plus two straight segments in the case A and plus four segments and an additional arc in case B.

The line that contain each segment is

$$x\,\frac{b_{2y} - b_{1y}}{L_b} - y\,\frac{b_{2x} - b_{1x}}{L_b} = \frac{b_{1x}(b_{2y} - b_{1y}) - b_{1y}(b_{2x} - b_{1x})}{L_b} + \eta\,\epsilon_{p_rp_gv} \quad (35)$$

where L_b is the nominal length of edge l_b and the components of $\vec{b}_1$ and $\vec{b}_2$ are calculated according to equation (7) with $\delta_{p_rp_gv} = 0$ and $\delta_{\phi_r\phi_g}$, as well as η, as described below.

In case A, one line is obtained for $\delta_{\phi_r\phi_g} = \epsilon_{\phi_r\phi_g}$ and selecting η equal to 1 or -1 to make the line tangent to the boundaries of *Uv* of $\vec{b}_1$ and *Uv* of $\vec{b}_2$, the points of tangency being the limits of the corresponding segment. The other line and segment are obtained in the same way taking $\delta_{\phi_r\phi_g} = -\epsilon_{\phi_r\phi_g}$.

In the case B, a pair of parallel lines are obtained considering $\delta_{\phi_r\phi_g} = \epsilon_{\phi_r\phi_g}$ and $\eta = 1, -1$, and another pair considering $\delta_{\phi_r\phi_g} = -\epsilon_{\phi_r\phi_g}$ and again $\eta = 1, -1$. One line of each pair is tangent to the additional arc (described below) and to *Uv* of $\vec{b}_1$ and *Uv* of $\vec{b}_2$, the points of tangency being the limits of the corresponding segments. The other two lines intersect each other and are respectively tangents to *Uv* of $\vec{b}_1$ and *Uv* of $\vec{b}_2$, the intersection point and each point of tangency being the limits of the two corresponding segments. Finally, the additional arc belongs to the circumference

$$\begin{cases} x = p_{r_x\circ} + (d_n - \epsilon_{p_rp_gv})\cos\theta_n \\ y = p_{r_y\circ} + (d_n - \epsilon_{p_rp_gv})\sin\theta_n \end{cases} \quad (36)$$

where d_n is the distance (without uncertainty) between l_b and the reference point, and satisfy

$$|\theta_n - \psi_{n_b}| < \epsilon_{\phi_g\phi_r} \quad (37)$$

with ψ_{n_b} indicating the direction of the external normal to l_b (Fig. 6).

Step 3. *CUl* is determined by applying a contact condition between *Ul* and the vertex $\vec{a}$. The boundary of *CUl* is obtained by equaling the boundary of *Ul* to the expression of $\vec{a}$ given by equation (5), and solving for the reference point. Due to the uncertainty of the position of $\vec{a}$ the result is a set of configurations whose external envelope conforms the boundary of *CUl*.

CUl has the same shape (but not same size) of *Ul* and therefore its boundary is composed by a similar set of arcs and segments.

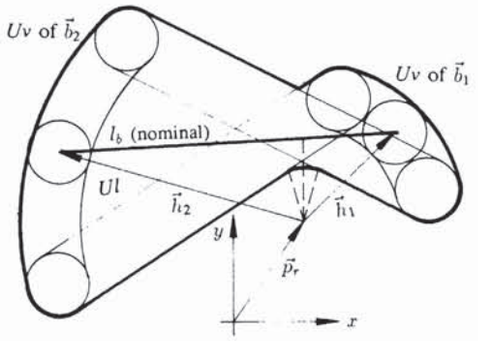

Figure 6: *Ul* of type-2 contact (case B)

They lie on the following circumferences and lines

$$\begin{cases} p_{r_x o} = a_{xo} + (h_i + \eta(\epsilon_{p_r p_g v} + \epsilon_a))\cos\theta_{R_{ra}} \\ p_{r_y o} = a_{yo} + (h_i + \eta(\epsilon_{p_r p_g v} + \epsilon_a))\sin\theta_{R_{ra}} \end{cases} \quad (38)$$

$$\begin{cases} p_{r_x o} = a_{xo} - h_i\cos(\phi_{ro} + \phi_{go} \pm \epsilon_{\phi_r \phi_g} + \gamma_i) \\ \qquad +(\epsilon_{p_r p_g v} + \delta_a)\cos\theta_{p_r p_g va} \\ p_{r_y o} = a_{yo} - h_i\sin(\phi_{ro} + \phi_{go} \pm \epsilon_{\phi_r \phi_g} + \gamma_i) \\ \qquad +(\epsilon_{p_r p_g v} + \delta_a)\sin\theta_{p_r p_g va} \end{cases} \quad (39)$$

the two circumferences given by (38) for $\eta = 1, -1$ are called CCr_M and CCr_m respectively. Likewise, those given by (39) are called CCg_M and CCg_m. For $\eta = -1$ the radius of a CCr_m could become negative, then CCr_m is not part of the boundary. Circumferences (39) and (39) are particularized for both vertices $\vec{b}_1$ and $\vec{b}_2$ by considering h_i and γ_i for $i = 1, 2$ respectively.

The straight lines tangents to these circumferences are

$$x\,\frac{b_{2y} - b_{1y}}{L} - y\,\frac{b_{2x} - b_{1x}}{L} = \frac{b_{1x}(b_{2y} - b_{1y}) - b_{1y}(b_{2x} - b_{1x})}{L} + \eta(\epsilon_{p_r p_g v} + \epsilon_a) \quad (40)$$

where η is chosen with the same criterion that in equation (35) for both cases A and B.

Finally, the circumference (36) becomes

$$\begin{cases} x = p_{r_x o} + (d_n - \epsilon_{p_r p_g v} - \epsilon_a)\cos\theta_n \\ y = p_{r_y o} + (d_n - \epsilon_{p_r p_g v} - \epsilon_a)\sin\theta_n \end{cases} \quad (41)$$

Step 4. As in type-1 C-surfaces, *CUl* is a two dimensional cut of *CU* for a certain o_{ro}. Then, again, the boundary of *CU* can be obtained from the boundary of *CUl* by varying o_{ro} within a given range.

Let L_{a1}, L_{a2}, L_b be the nominal lengths of edges l_{a1}, l_{a2} and l_b (l_{a1} and l_{a2} are the edges that joint in $\vec{a}$ following the object boundary counterclokwise). The maximum deviations of the corresponding external normal directions are

$$\epsilon_{v_{n_{a1}}} = 2\epsilon_a / L_{a1} \quad (42)$$

$$\epsilon_{v_{n_{a2}}} = 2\epsilon_a / L_{a2} \quad (43)$$

$$\epsilon_{v_{n_b}} = 2\epsilon_a / L_b \quad (44)$$

The variation range of o_{ro} will be extended, due to uncertainty, to

$$\phi_{ro_m} - \epsilon_{v_{n_{a1}}} - \epsilon_{v_{n_a}} - \epsilon_{\phi_r} - \epsilon_{\phi_g} < \phi_{ro} < \phi_{ro_M} + \epsilon_{v_{n_{a2}}} + \epsilon_{v_{n_a}} + \epsilon_{\phi_r} + \epsilon_{\phi_g} \quad (45)$$

CONCLUSIONS

Uncertainty sources affecting contact between an object fixed in the robot gripper and any object in the work environment are described, and an uncertainty model for each source has been proposed. These models are used to determine the boundary of the Configuration Space subset (*CU*) in which a given contact is possible due to uncertainty. By this way, uncertainty in the real world is mapped into the Configuration Space.

In robot motion planning in presence of uncertainty, subsets *CU* will be considered instead of the nominal C-surfaces. In obstacle avoidance movements, robot trajectories must not contain configurations within any *CU* (gross motion); on the contrary, in assembly, robot trajectories will necessary pass through at least one *CU* (fine motion), and undesirable contacts may occur there.

Uncertainty has been modelled for the three degrees of freedom of planar movements, but it can be extended to more degrees of freedom without theoretical problems.

REFERENCES

Benhabib B., R. Fenton and A. Goldenberg (1987). Computer-Aided Joint Error Analysis of Robots. *IEEE Journal of Robotics and Automation*, Vol.RA-3 (4), 317-322.

Brooks R. A. Symbolic Error Analysis and Robot Planning (1989). *The International Journal of Robotics Research*, Vol.1 (4), 29-68.

Buckley S. J. (1987). Planning and Teaching Compliant Motion Strategies. *MIT Artificial Intelligence Laboratory report AI-TR-936 (Ph.D Thesis)*.

Day C. (1988). Robot Accuracy Issues and Methods of Improvement. *Robotics Today*, Vol.1 (1), 1-9.

Donald B. R. (1988). A Geometric Approach to Error Detection and Recovery for Robot Motion Planning with Uncertainty. *Artificial Intelligence*, Num.37, 223-271.

Fleming A.D. (1989). A Representation for Geometric Toleranced Parts. In John Woodwark (Ed.), *Geometric Reasoning*, Chapter 9, Clarendon Press, Oxford. pp. 141-168.

Jayaraman R. and V. Srinivasan (1989). Geometric toleranc-ing: I. Virtual boundary requirements. *IBM Journal Research Development*, Vol.33 (2), 90-104.

Lozano Perez, T. (1983). Spatial planning: a configuration space approach. *IEEE Trans. on Computers, C-32* (2), 108-120.

Requicha, A.A. (1983). Toward a theory of geometric tolerancing. *The Int. Journal of Robotics Research, 4* (2), 45-60.

Suárez R. and L. Basañez (1989). Automatic Fine-Motion Planning based on Position/Force States. *Preprints of IFAC Symposium INCOM'89*, Madrid, Spain, 369-375.

Xiao J., R. Volz (1988). Design and Motion Constraints of Part-Mating Planning in the Presence of Uncertainties. *Proceedings of the 1988 IEEE Int. Conf. on Robotics and Automation*, Philadelphia, USA, 1260-1268.